QUANTUM HADRODYNAMICS*

Brian D. Serot**
Physics Department and Nuclear Theory Center
Indiana University
Bloomington, IN 47405

INTRODUCTION

The traditional approach to nuclear structure is based on the Schroedinger equation and involves nucleons interacting through static, two-body potentials. Since this equation can be solved exactly for two nucleons, empirical nucleon-nucleon (NN) data is used to constrain the two-body potential. One then attempts to (approximately) solve the many-body problem to describe atomic nuclei. This approach has been very successful and has taught us much about nuclear structure; nevertheless, there are several reasons why it is inadequate for a detailed understanding of nuclear systems.

For example, there is now convincing evidence that the NN interaction contains large Lorentz scalar and four-vector components.[1-9] This has two immediate consequences for the nuclear many-body problem. First, since the resulting single-particle potentials in a nucleus are comparable to the nucleon mass, relativistic effects can be important at low energies and ordinary densities. In particular, the strong scalar field enhances the lower components of the Dirac wave function of a nucleon, leading implicitly to significant velocity, spin, and density dependence in the nucleon-nucleus interaction.[3,4,8-12] In addition, strong interactions introduce a new energy scale into nuclear matter calculations that is approximately several hundred MeV at ordinary densities. The nuclear matter binding energy now involves not only the familiar cancellation between average kinetic and potential energies, but also a delicate cancellation between large attractive and repulsive contributions to the potential energy. The validity of nonrelativistic calculations of nuclear matter saturation must therefore be re-examined so that their apparent successes can be better understood.

There are other reasons for developing a relativistic nuclear many-body theory. To calculate the properties of condensed stellar objects and to predict the outcome of collisions between energetic heavy ions, one requires the nuclear matter equation of state at temperatures and densities far removed from the regime of ordinary nuclei. In these extreme situations, relativistic propagation of the nucleons, retardation in the interaction, and the causal propagation of signals are important physical constraints. It is also necessary to introduce the mesonic degrees of freedom that mediate the nucleon-nucleon interaction, since their production and absorption may

* Supported in part through U.S. Department of Energy contract DE-AC02-81ER40047.
** Alfred P. Sloan Foundation Research Fellow.

play a major role under the extreme conditions mentioned above. Indeed, there is now conclusive evidence that meson and baryon degrees of freedom (including baryon resonances) are relevant even in ordinary nuclei, as illustrated by meson-exchange currents in electron scattering from nuclei at momentum transfers of several hundred MeV.[13]

The only existing framework that provides a consistent description of these relativistic meson-baryon systems is relativistic quantum field theory based on a local lagrangian density. We will call these theories "quantum hadrodynamics" or QHD. There are several important reasons for using a formalism based solely on hadrons. First, these appear to be the relevant degrees of freedom for nuclear processes at low to medium energies; they are also the objects actually observed in experiments, as quarks and gluons appear to be confined. Second, although the internal quark-gluon substructure of hadrons may be visible under very extreme conditions (for example, in a nuclear matter phase transition to a quark-gluon plasma), it is still important to have a consistent description of matter in the hadronic phase. Finally, the only way to unamibiguously identify explicit signals of quantum chromodynamic (QCD) behavior in nuclear processes is through an inadequacy in the predictions of QHD.

It is important to formulate QHD using renormalizable lagrangian densities. This allows for consistent calculations at any desired level of approximation. The results can be expressed in terms of a finite number of parameters (coupling constants and masses). Renormalizable models also allow for studies of the dynamical quantum vacuum (for example, virtual $N\bar{N}$ pairs) in the nuclear medium. Moreover, since renormalizable QHD does not require additional ad hoc cutoff procedures, it is the least sensitive to the high-momentum (short-distance) behavior of the hadronic interaction. This input may or may not provide a satisfactory description of nuclear matter under all of the conditions mentioned above; nevertheless, it can be tested and its limitations discovered as with all questions in physics--through a detailed comparison between consistent theoretical results and experimental measurements.

Quantum hadrodynamics is a general framework for the relativistic nuclear many-body problem.[14] The detailed dynamics must be specified by choosing a particular renormalizable lagrangian density. In the present work, we review some applications of QHD to nuclear matter and finite nuclei, focusing primarily on the consequences of the Lorentz structure of the NN interaction. It is therefore useful to begin with the Walecka model,[10] which contains baryons (ψ) and neutral scalar (ϕ) and vector (V_μ) mesons. This model is called QHD-I in ref. 14. The lagrangian density is given by

$$\mathcal{L} = \bar{\psi}\left[\gamma_\mu(i\partial^\mu - g_V V^\mu) - (M - g_S\phi)\right]\psi + \frac{1}{2}(\partial_\mu\phi\partial^\mu\phi - m_S^2\phi^2) - \frac{1}{4}(\partial_\mu V_\nu - \partial_\nu V_\mu)^2 + \frac{1}{2}m_V^2 V_\mu V^\mu + \text{counterterms} \qquad (1)$$

where the conventions are those of refs. 14 and 15. The parameters M, g_S, g_V, m_S, and m_V are phenomenological constants that may be determined (in principle) from

experimental measurements. The counterterms are for renormalization purposes, as discussed below.

The present motivation for this model comes from the empirically observed large Lorentz scalar and four-vector components in the NN interaction. These must, of course, be reproduced in any relativistic theory of nuclear structure, and the simplest way to do this is through the exchange of scalar and vector mesons. The other Lorentz components of the NN interaction (pseudoscalar, tensor, and axial vector) average essentially to zero in spin-saturated nuclear matter and may be incorporated as refinements to the present model.[14] Since the lagrangian (1) resembles massive quantum electrodynamics with an additional scalar interaction, this model is renormalizable.

MEAN-FIELD THEORY

The Euler-Lagrange equations resulting from eq. (1) are

$$(\partial_\mu \partial^\mu + m_s^2)\phi = g_s \bar{\psi}\psi \tag{2}$$

$$\partial_\nu(\partial^\nu V^\mu - \partial^\mu V^\nu) + m_v^2 V^\mu = g_v \bar{\psi}\gamma^\mu \psi \tag{3}$$

$$\left[\gamma^\mu(i\partial_\mu - g_v V_\mu) - (M - g_s\phi)\right] \psi = 0 \tag{4}$$

These are nonlinear quantum field equations, and their exact solutions are very complicated. In particular, they describe mesons and baryons that are not point particles, but rather objects with intrinsic structure due to the implied (virtual) meson and baryon-antibaryon loops. Moreover, since we expect the couplings g_s and g_v to be large, perturbative solutions are not useful. Fortunately, there exists an approximate solution that should become increasingly valid as the nuclear density increases; it may be obtained by replacing the meson field operators and baryon sources with their classical expectation values. In infinite matter, the resulting classical meson fields ϕ_0 and V_0 are uniform and constant, and they satisfy

$$\phi_0 = \frac{g_s}{m_s^2} \langle\bar{\psi}\psi\rangle \equiv \frac{g_s}{m_s^2}\rho_s \tag{5}$$

$$V_0 = \frac{g_v}{m_v^2} \langle\psi^\dagger\psi\rangle \equiv \frac{g_v}{m_v^2}\rho_B = \frac{g_v}{m_v^2}\left(\frac{\xi}{3\pi^2}k_F^3\right) \tag{6}$$

Note that $\langle \underset{\sim}{V} \rangle = 0$ by rotational invariance. Here k_F is the Fermi wavenumber and ξ is the isospin degeneracy: $\xi = 1$ for neutron matter, $\xi = 2$ for nuclear matter.

When the classical meson fields of eqs. (5) and (6) are substituted into eq. (4) for the Dirac field, that equation is linear,

$$\left[i\gamma_\mu\partial^\mu - g_v\gamma^0 V_0 - (M - g_s\phi_0)\right]\psi = 0 \tag{7}$$

and can be solved exactly. (It is this linearization of the full field equation (4) that allows the baryons to be interpreted now as point particles.) The resulting baryon solutions have a mass that is shifted by the scalar field:

$$M^* \equiv M - g_s\phi_0 \tag{8}$$

and an energy spectrum that is shifted by the vector field:

$$E^{(\pm)}(k) = g_v V_0 \pm (\underset{\sim}{k}^2 + M^{*2})^{1/2} \equiv g_v V_0 \pm E^*(k) \tag{9}$$

As expected, there are solutions with both positive and negative square roots characteristic of the Dirac equation. Denoting these by solutions by $U(\underset{\sim}{k},\lambda)$ and $V(\underset{\sim}{k},\lambda)$, respectively, we find

$$U(\underset{\sim}{k},\lambda) = N(k)\begin{pmatrix} 1 \\ \dfrac{\underset{\sim}{\sigma}\cdot\underset{\sim}{k}}{E^*(k)+M^*} \end{pmatrix} X_\lambda \; ; \; V(\underset{\sim}{k},\lambda) = N(k) \begin{pmatrix} \dfrac{\underset{\sim}{\sigma}\cdot\underset{\sim}{k}}{E^*(k)+M^*} \\ 1 \end{pmatrix} X_\lambda \tag{10}$$

where X_λ is a two-component Pauli spinor and $N(k)$ is a normalization factor.

These solutions can be used to define quantum field operators, and the hamiltonian for the system can be constructed in the canonical fashion.[14] The result is

$$\hat{H} = \hat{H}_{MFT} + \delta H \tag{11}$$

$$\hat{H}_{MFT} = g_v V_0 \hat{B} + \sum_{\underset{\sim}{k}\lambda} E^*(k)\left[A^\dagger_{\underset{\sim}{k}\lambda}A_{\underset{\sim}{k}\lambda} + B^\dagger_{\underset{\sim}{k}\lambda}B_{\underset{\sim}{k}\lambda}\right] + V\left[\tfrac{1}{2}m_s^2\phi_0^2 - \tfrac{1}{2}m_v^2V_0^2\right] \tag{12}$$

$$\hat{B} = \sum_{\underset{\sim}{k}\lambda}\left[A^\dagger_{\underset{\sim}{k}\lambda}A_{\underset{\sim}{k}\lambda} - B^\dagger_{\underset{\sim}{k}\lambda}B_{\underset{\sim}{k}\lambda}\right] \tag{13}$$

$$\delta H = -\sum_{\underset{\sim}{k}\lambda}\left[(\underset{\sim}{k}^2 + M^{*2})^{1/2} - (\underset{\sim}{k}^2 + M^2)^{1/2}\right] \tag{14}$$

Here $A^\dagger_{\underset{\sim}{k}\lambda}$, $B^\dagger_{\underset{\sim}{k}\lambda}$, $A_{\underset{\sim}{k}\lambda}$, and $B_{\underset{\sim}{k}\lambda}$ are creation and destruction operators for (quasi)baryons and (quasi)antibaryons with shifted mass and energy, and V is the quantization volume. $\hat{B}$ is the baryon number operator, which clearly counts the number of baryons minus the number of antibaryons. (The index λ denotes both spin and isospin projections.) The correction term δH arises from placing the operators in $\hat{H}_{MFT}$ in normal order.[14] This correction is easily interpreted in the context of Dirac "hole theory." The spectrum of the infinite Dirac sea of occupied negative-energy states shifts in the presence of the surrounding nucleons at finite density. Since all energies are measured relative to the vacuum, the energy shift must be computed by subtracting the total energy of the Dirac sea in the vacuum, where the nucleons have their free mass M. This leads to the result in eq. (14). Here we will concentrate on the mean-field-theory (MFT) hamiltonian of eq. (12); the "vacuum fluctuation" correction δH will be discussed below.

Since the MFT hamiltonian $\hat{H}_{MFT}$ is diagonal, we have solved this model problem exactly. Thus the energy density for an infinite system of baryons with filled states up to Fermi wavenumber k_F may be readily evaluated:

$$\mathcal{E}_{MFT} = \frac{g_v^2}{2m_v^2}\rho_B^2 + \frac{m_s^2}{2g_s^2}(M - M^*)^2 + \frac{\xi}{\pi^2}\int_0^{k_F} t^2 E^*(t)\, dt \tag{15}$$

Here V_0 has been eliminated in terms of the conserved baryon density using eq. (6), and eq. (8) serves to eliminate ϕ_0. The effective mass M* must be determined by solving eq. (5) or, equivalently, by minimizing $\mathcal{E}_{MFT}$ with respect to M*, leading to the self-consistency relation

$$M^* = M - \frac{g_s^2}{m_s^2}\rho_s = M - \frac{g_s^2}{m_s^2}\frac{\xi}{\pi^2}\int_0^{k_F} t^2\, dt\, \frac{M^*}{E^*(t)} \tag{16}$$

Note that the scalar density ρ_s is smaller than the baryon density ρ_B due to the factor of M*/E*(t), which is an effect of Lorentz contraction. Thus the contribution of rapidly moving baryons to the scalar source is significantly reduced. Most importantly, eq. (16) is a transcendental self-consistency equation for M* that must be solved at each value of k_F. This illustrates the nonperturbative nature of the MFT solution.

The pressure may be defined by the thermodynamic relation

$$p = \rho_B^2 \frac{\partial}{\partial \rho_B}\left(\frac{\mathcal{E}}{\rho_B}\right) \tag{17}$$

$$P_{MFT} = \frac{g_v^2}{2m_v^2}\rho_B^2 - \frac{m_s^2}{2g_s^2}(M - M^*)^2 + \frac{1}{3}\frac{\xi}{\pi^2}\int_0^{k_F} dt\, \frac{t^4}{E^*(t)} \tag{18}$$

It can be readily verified that this expression agrees with that obtained from the (normal-ordered) energy-momentum tensor.[10,16]

An examination of the energy density shows that the system is unbound ($\mathcal{E}_{MFT}/\rho_B > M$) at either very high or very low densities.[10,14] At intermediate densities, the attractive scalar interaction will dominate if the coupling constants are chosen properly. The system then saturates. The empirical equilibrium properties of symmetric (N = Z) nuclear matter will be reproduced if the couplings are chosen as

$$C_s^2 \equiv g_s^2\,(M^2/m_s^2) = 267.1 \tag{19}$$

$$C_v^2 \equiv g_v^2\,(M^2/m_v^2) = 195.9 \tag{20}$$

which leads to an equilibrium Fermi wavenumber $k_F^0 = 1.42\ \mathrm{fm}^{-1}$ and an energy/nucleon ($\mathcal{E}_{MFT}/\rho_B - M$) = -15.75 MeV. (This somewhat large saturation density is chosen to present results consistent with those in refs. 10 and 14.) Note that only the ratios of coupling constants to masses enter in eqs. (15), (16), and (18). The resulting saturation curve is shown in fig. 1. For reasonable values of the meson masses (see table I), the resulting coupling constants g_s and g_v are similar to those obtained in

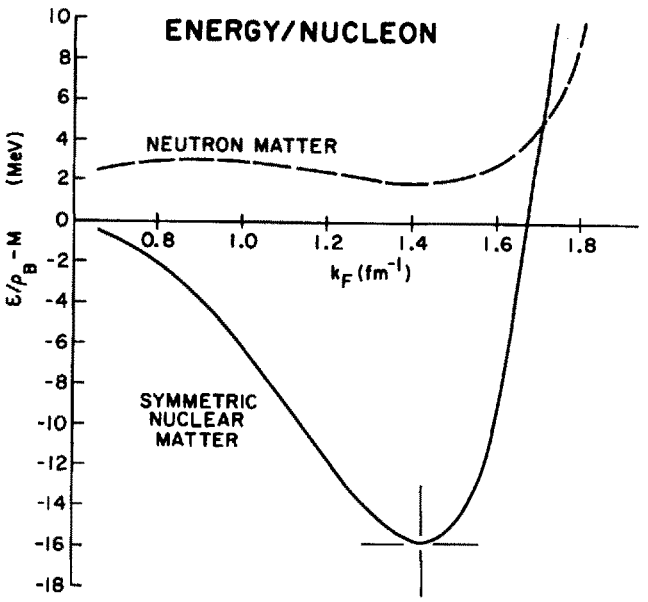

Fig. 1 Energy/nucleon in infinite matter in the mean-field approximation.

Table I

Model Parameters and Results

	g_s^2	g_v^2	M*/M	K(MeV)
mean field	91.64	136.2	0.56	540
mean field + vacuum fluctuations	62.89	79.78	0.72	470
Hartree-Fock	83.11	108.1	0.53	580

The meson masses used to derive these values are m_s = 550 MeV and m_v = 783 MeV. Each parameter set leads to nuclear matter saturation at k_F^0 = 1.42 fm^{-1} with binding energy 15.75 MeV in the indicated approximation. The HF value of M* ≡ M + $\Sigma^S(k)$ is evaluated at k = k_F^0. K is the compressibility.

one-boson-exchange-potential fits to NN scattering.[1,2] This implies that the dominant features of the observed NN interaction relevant for nuclear matter are qualitatively reproduced by the preceding normalization conditions.

Once the parameters have been specified, the properties of infinite matter in this approximation are determined for all densities, temperatures, and proton fractions Z/N. For example, the energy/nucleon in neutron matter ($\xi = 1$) is also shown in fig. 1.

The self-consistent effective mass M* is shown in fig. 2. Observe that M*/M is significantly less than unity at ordinary nuclear densities. This is a consequence of the large condensed scalar field $g_s\phi_0$, which is approximately 400 MeV and provides a large attractive contribution to the energy/nucleon. There is a corresponding large repulsive energy/nucleon from the vector field $g_v V_0 \simeq 350$ MeV. Thus the Lorentz structure of the interaction introduces a new energy scale in the problem, and the small nuclear binding energy ($\simeq$ 16 MeV) arises from the cancellation between the large scalar attraction and vector repulsion. Note also that the significant shift in the nucleon mass is a new physical effect that is not present in calculations based on static nonrelativistic potentials. Indeed, in this approximation, it is the shift in the nucleon mass and the relativistic properties of the scalar and vector fields that are responsible for saturation; a Hartree-Fock variational estimate built on the nonrelativistic potential limit of the interaction shows that such a system is unstable against collapse.[17]

Because of the sensitive cancellations involved near the equilibrium density, corrections to the MFT must ultimately be considered. These may be calculated systematically in the framework of QHD.[14] Nevertheless, the Lorentz structure of the interaction provides an additional saturation mechanism that is not present in the nonrelativistic potential limit.

The corresponding curves for neutron matter (obtained by setting $\xi = 1$) are also shown in figs. 1 and 2, and the equation of state (pressure vs. energy density) for neutron matter at all densities is given in fig. 3. In this model, there is a phase transition similar to the liquid--gas transition in the van der Waals' equation of state, and the properties of the two phases are deduced through a Maxwell construction. At high density, the system approaches the causal limit $p = \mathcal{E}$, representing the "stiffest" possible equation of state; this asymptotic regime is already relevant at densities in the interiors of neutron stars ($\mathcal{E} \simeq 10^{15}$ g/cm^3).[15,18] Although the low-density behavior of nuclear matter is sensitive to the cancellation between scalar and vector components, the scalar field approaches a limiting value ($g_s\phi_0 \to M$) at high densities (see fig. 2), resulting in (essentially) massless baryons interacting through a strong vector repulsion.[10,14] Thus, regardless of the precise values of the scalar and vector masses and couplings, the stiff high-density equation of state is determined by the Lorentz structure of the interaction. Moreover, because the individual Lorentz components are comparable to the nucleon mass, the onset of the

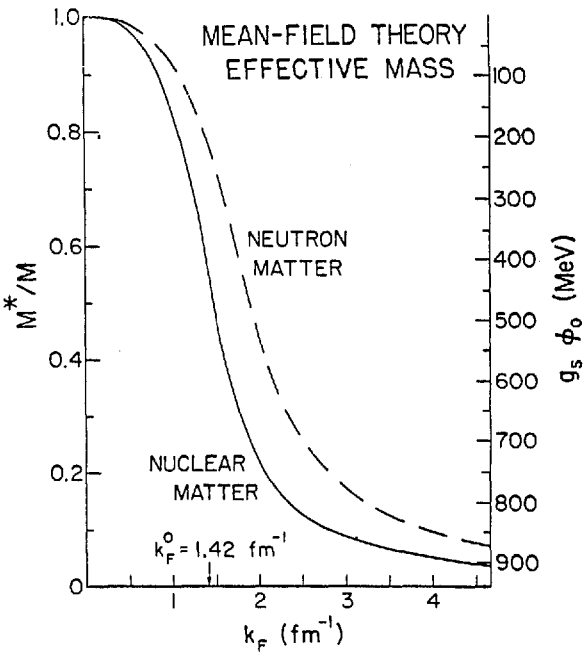

Fig. 2 Mean-field effective mass $M^* = M - g_s\phi_0$ in infinite nuclear matter.

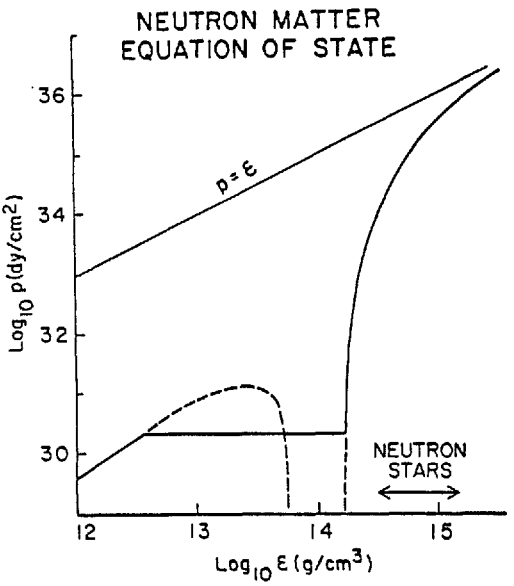

Fig. 3 Neutron matter equation of state in the mean-field approximation.

asymptotic regime occurs at modest densities ($\mathcal{E} \simeq 10^{15}$ g/cm^3). The importance of relativistic effects in this regime implies that the extrapolation of nonrelativistic nuclear matter calculations to these densities is questionable.

RELATIVISTIC HARTREE THEORY OF NUCLEI

The preceding formalism can be extended to describe spherically symmetric closed-shell nuclei by allowing the classical meson fields to acquire a spatial dependence.[3-5] The fields are still determined by local sources, but the sources are now computed using baryon wave functions that are solutions to the Dirac equation in the spatially dependent meson fields. Thus the scalar and vector fields are determined by the differential equations

$$(\nabla^2 - m_s^2)\phi_0(r) = -g_s\rho_s(r) \equiv -g_s \sum_{\alpha}^{occ} \bar{\psi}_\alpha(\underset{\sim}{x})\psi_\alpha(\underset{\sim}{x}) \tag{21}$$

$$(\nabla^2 - m_v^2)V_0(r) = -g_v\rho_B(r) \equiv -g_v \sum_{\alpha}^{occ} \psi_\alpha^\dagger(\underset{\sim}{x})\psi_\alpha(\underset{\sim}{x}) \tag{22}$$

where the sum runs over occupied single-particle states. As in the MFT of the previous section, only contributions from positive-energy ("valence") nucleons are included. Corrections from the filled Dirac sea that defines the quantum vacuum will be discussed in the next section.

The ground state of the nucleus is a product of relativistic single-particle wave functions describing nucleons moving in the condensed meson fields. Each nucleon satisfies the Dirac equation

$$\left[-i\underset{\sim}{\alpha}\cdot\underset{\sim}{\nabla} + g_v V_0(r) + \beta(M - g_s\phi_0(r))\right]\psi_\alpha(\underset{\sim}{x}) = E_\alpha\psi_\alpha(\underset{\sim}{x}) \tag{23}$$

and has a shifted mass that is spatially dependent. The nuclear ground state is thus described by coupled nonlinear differential equations that are to be solved <u>self-consistently</u> (for example, by iteration).

The preceding relativistic Hartree equations for finite nuclei are correct in QHD-I. For comparing quantitative predictions with experiment, however, it is necessary to extend the description to include rho mesons and the coulomb field. A renormalizable model ("QHD-II") containing these fields is discussed in ref. 14, and the full Hartree equations are illustrated there. Note that since the nucleus has well-defined charge Z, only <u>neutral</u> meson fields have classical counterparts and appear in these equations. In addition, there is no condensed field for the (pseudoscalar) pion, since the nuclear ground state has well-defined parity and is spherically symmetric.

Since the meson masses and coupling constants appear separately in these equations, there are four free parameters in model QHD-II: the σ (scalar), ω (vector), and ρ meson coupling constants, and the σ meson mass m_s. The remaining parameters (nucleon mass,

ω and ρ meson masses, and the fine-structure constant α) are set equal to their experimental values. The free parameters are determined as in ref. 4 from the binding energy, symmetry energy, and equilibrium saturation density of nuclear matter (the value $k_F^0 = 1.30$ fm^{-1} is used), and the rms charge radius in ^{40}Ca. Once this is done, the properties of all closed-shell nuclei are determined in this approximation. For example, figs. 4 and 5 show the relativistic charge densities of ^{40}Ca and ^{208}Pb compared with two nonrelativistic calculations and the empirical distributions determined from elastic electron scattering.[4] Similar results are obtained for other closed shell nuclei. Here the empirical proton form factor is folded with the calculated "point proton" density to determine the charge density, as discussed in refs. 4 and 19.

Figure 6 compares the predicted energy levels in ^{208}Pb with experimental values derived from neighboring nuclei.[20,21] The relativistic Hartree calculations clearly reveal a shell structure. This arises from the spin-orbit interaction that occurs naturally when a Dirac particle moves in large classical scalar and vector fields.[3,4] Thus, with a minimal number of phenomenological parameters determined from bulk nuclear properties, one derives the existence of the nuclear shell model.

There are several advantages to the present model of nuclear structure. First, the calculation of the nuclear ground state is self-consistent. The condensed scalar and vector fields follow directly from the scalar and baryon densities, which are in turn determined by the solutions to the Dirac equation (23) in the condensed fields.

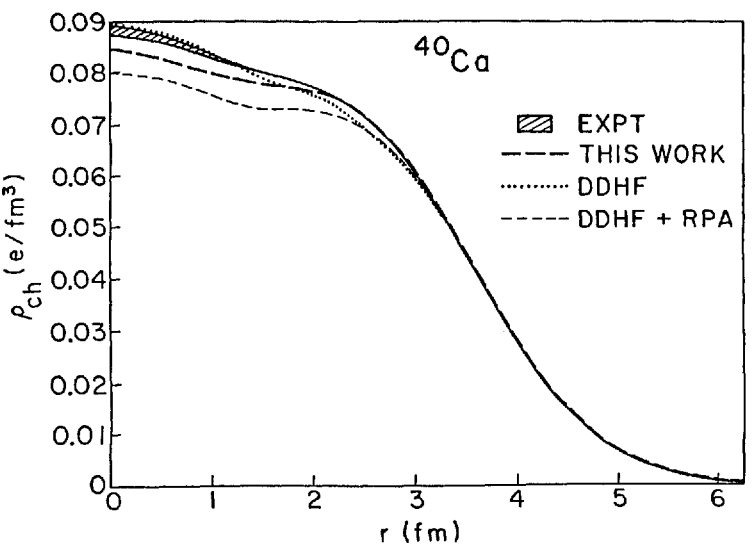

Fig. 4 Charge density distributions for ^{40}Ca.[4] The experimental curve is from ref. 37. The density-dependent Hartree-Fock (DDHF) results are those of Negele, and the DDHF + RPA calculation is that of Gogny, as indicated in ref. 37. The relativistic Hartree calculations yield the long-dashed curve.

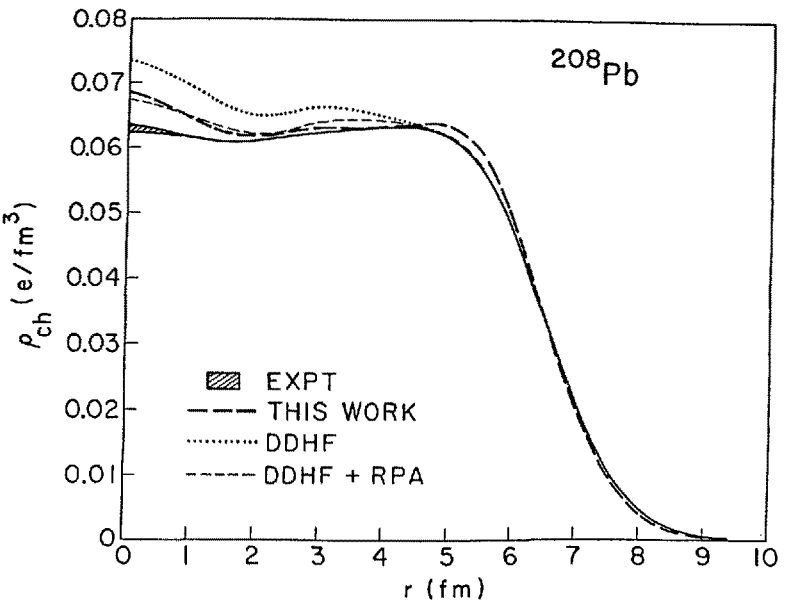

Fig. 5 Charge density distributions for ^{208}Pb.[4] The solid curve and shaded area represent the fit to the experimental data given in ref. 38. Relativistic Hartree results are indicated by the long-dashed line. The density-dependent Hartree-Fock calculations of Gogny[39] are denoted by the dotted (DDHF) and short-dashed (DDHF + RPA) curves.

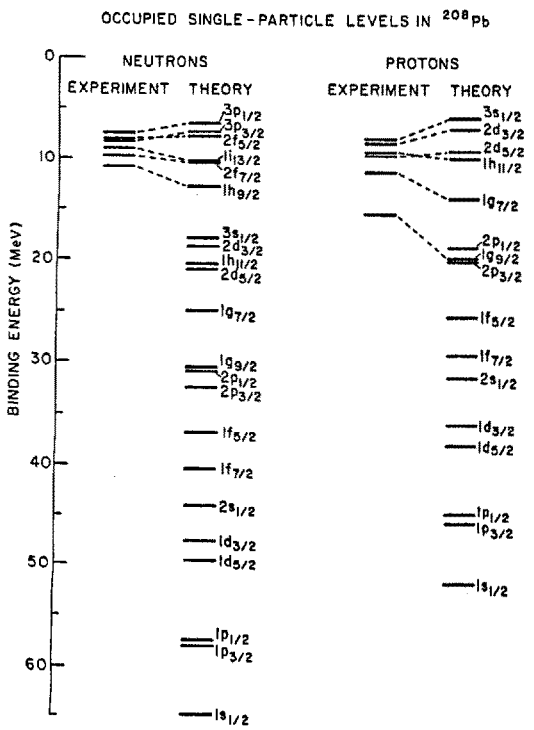

Fig. 6 Predicted spectrum for occupied levels in ^{208}Pb. Experimental levels are from neighboring nuclei.[20,21]

Second, one set of parameters specifies all closed-shell nuclei in this approximation. Finally, this relativistic shell model is simply one piece of a complete many-body framework based on QHD. One can therefore systematically investigate corrections to the nuclear ground state (like those arising from nucleon exchange or two-nucleon correlations) or compute excited states using a residual particle-hole interaction derived from the same QHD lagrangian.[22] In addition, since the underlying theory is renormalizable, one can examine corrections from the filled Dirac sea of negative-energy states, as discussed in the following section.

CORRECTIONS TO THE MEAN-FIELD THEORY

One advantage of quantum hadrodynamics is that it provides a consistent framework for studying corrections to the MFT. In this section, we examine three classes of corrections: vacuum fluctuations, self-consistent nucleon exchange, and two-nucleon correlations. We will concentrate primarily on model QHD-I.

The mean-field hamiltonian $\hat{H}_{MFT}$ is defined by a normal-ordering procedure. This isolates contributions to the energy arising from the filled Dirac sea of negative-energy states [see eqs. (11)--(14)]. Since the baryon mass becomes M* at finite density, the spinors describing the negative-energy solutions also have a shifted mass [eq. (10)]. The resulting shift in the spectrum of the negative-energy states relative to the vacuum leads to a "vacuum fluctuation" correction to the energy, as written in eq. (14). The sum over all negative-energy states leads formally to an infinite result. Since the present model is <u>renormalizable</u>, however, this result may be rendered finite by adding the appropriate counterterms and imposing a set of renormalization conditions. This procedure is described in detail in refs. 14, 16, and 23 and results in a correction to the MFT energy density

$$\Delta\mathcal{E}_{vac} = -\frac{1}{V}\sum_{\underset{\sim}{k}\lambda}\left[(\underset{\sim}{k}^2 + M^{*2})^{1/2} - (\underset{\sim}{k}^2 + M^2)^{1/2}\right] + \sum_{n=1}^{4}\frac{c_n}{n!}(\phi_0)^n \tag{24}$$

$$= -\frac{1}{4\pi^2}\left[M^{*4}\ln(M^*/M) + M^3(M - M^*) - \frac{7}{2}M^2(M - M^*)^2 + \frac{13}{3}M(M - M^*)^3 - \frac{25}{12}(M - M^*)^4\right] \tag{25}$$

Here the counterterm contributions are shown explicitly in eq. (24) as a <u>finite</u> polynomial in the condensed scalar field. The total energy density is now given by the sum of eqs. (15) and (25), and the new self-consistent M* is determined by minimizing the result with respect to M*. This is again equivalent to solving the scalar field equation (5), including the correction to ρ_s coming from the shifted mass of the negative-energy states. This is given by [14]

$$\Delta\rho_s^{vac} \equiv \partial(\Delta\mathcal{E}_{vac})/\partial M^* = -\frac{1}{\pi^2}\left[M^{*3}\ln(M^*/M) + \frac{1}{3}M^3 - \frac{3}{2}M^2M^* + 3MM^{*2} - \frac{11}{6}M^{*3}\right] \quad (26)$$

We emphasize that the corrections (24)--(26) are insensitive to the short-distance structure of the baryons, as they arise solely from the change in the baryon mass in the presence of the uniform scalar field.

To discuss the size of the vacuum fluctuation corrections, we use two different procedures. First, in table I we compare the values of the coupling constants that reproduce the empirical nuclear matter saturation properties. Observe that g_s and g_v change by only $\simeq$ 25% when the fluctuation corrections are included. After renormalization, the baryon effective mass M* and nuclear matter compressibility $K \equiv 9\rho_B^2(\partial^2\mathcal{E}/\partial\rho_B^2)$ differ at about the same level in the two approximations. The new value of M* implies that the large scalar and vector fields change by $\simeq$ 35%.

As a second way to examine corrections, we compare predicted quantities using a fixed set of parameters determined from the MFT results and given in the first row of table I. Figures 7 and 8 show the energy/nucleon and equation of state (EOS) for the present approximations. Observe that the equilibrium Fermi wavenumber k_F^0 shifts by $\simeq 0.25\ fm^{-1}$, and the binding energy changes by $\simeq$ 10 MeV when the fluctuations are included. Although the latter is small compared to the large scalar and vector fields ($\simeq$ 300 MeV), the modification to the binding energy is significant, reflecting the sensitive cancellation between attractive and repulsive components in the potential energy. The vacuum fluctuation corrections are a direct consequence of a relativistic treatment of the nuclear many-body problem and are absent in a nonrelativistic approach. The nuclear matter EOS at low densities also changes because the saturation point is different in the two approximations, but for $\mathcal{E} \gtrsim 0.5\ GeV/fm^3 \simeq 10^{15}\ g/cm^3$, the corrected results are essentially in agreement with the MFT, signaling the dominance of the vector repulsion and the onset of a stiff equation of state.

These vacuum fluctuation corrections also modify the structure of a finite nucleus.[24] To examine these effects, let $\rho_s \to \rho_s + \Delta\rho_s^{vac}$ in eq. (21) for the scalar field, using eq. (26) for $\Delta\rho_s^{vac}$. The radial dependence of $\Delta\rho_s^{vac}$ is achieved through the local-density approximation by taking $M^* \equiv M^*(r) = M - g_s\phi_0(r)$. Since $\Delta\rho_s^{vac}$ now depends explicitly on $\phi_0(r)$, the modified eq. (21) becomes a nonlinear differential equation.

Results for finite nuclei may now be obtained by solving the coupled relativistic Hartree equations discussed above, including the modifications to eq. (21). The model parameters are renormalized ("re-fit") using the same input as in the original Hartree case.[24] With these normalization conditions, the calculated charge and baryon densities are essentially equal to those in the original Hartree approximation, as indicated in fig. 9 for ^{208}Pb; the effects in lighter nuclei are even smaller. Note, however, that the vacuum correction reduces the scalar density relative to the baryon density; in the present case, the former is approximately 85% of the latter in the

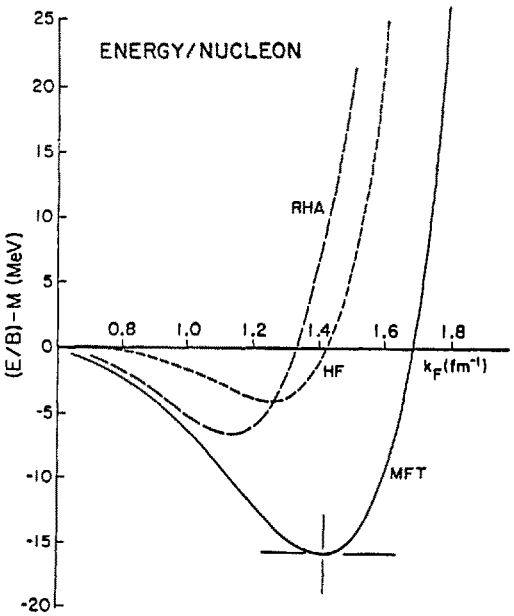

Fig. 7 Energy/nucleon in nuclear matter for the mean-field theory (solid), relativistic Hartree-Fock (short dashes), and mean field plus vacuum fluctuations (long dashes). All results use parameters from the first row in table I.

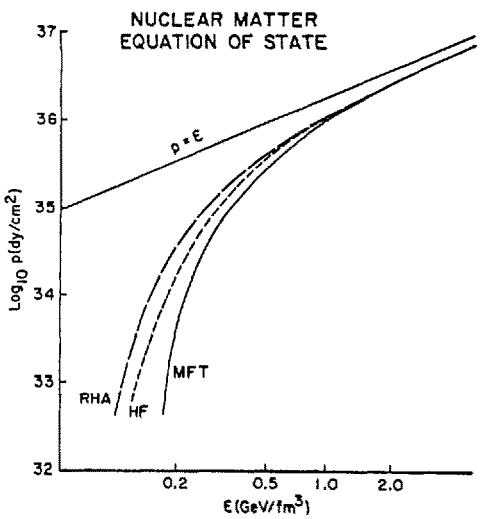

Fig. 8 Nuclear matter equation of state. The curves are calculated and labeled as in fig. 7.

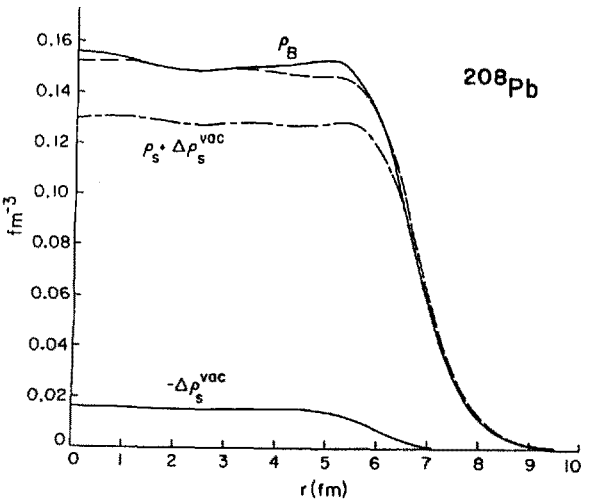

Fig. 9 Density profiles in ^{208}Pb. The total baryon density ρ_B shown by the solid curve is calculated in the relativistic Hartree approximation without vacuum fluctuations. The corresponding result including vacuum fluctuations is given by the dashed curve. Also shown are the total scalar density $\rho_s + \Delta\rho_s^{vac}$ and (minus) the vacuum fluctuation correction $-\Delta\rho_s^{vac}$. All curves are "point" densities that do not include single-nucleon form factors.

nuclear interior, as compared with 93% in the simple Hartree approximation. Preliminary relativistic impulse approximation calculations[25] show that this difference may be detectable in medium-energy nucleon-nucleus scattering.

We turn now to corrections from nucleon exchange, which are incorporated in the relativistic Hartree-Fock (HF) approximation.[26,27] Begin by examining the proper baryon self-energy $\Sigma(k)$ in the nuclear medium, which can be written as[14]

$$\Sigma(k) = \Sigma^S(k) - \gamma_\mu\Sigma^\mu(k) = \Sigma^S(k) - \gamma^0\Sigma^0(k) + \underset{\sim}{\gamma}\cdot\underset{\sim}{k}\,\Sigma^V(k) \tag{27}$$

In the MFT, Σ^S and Σ^0 become momentum-independent constants $-g_s\phi_0$ and $-g_v V_0$, and Σ^V vanishes. In the HF approximation, $\Sigma(k)$ is calculated by summing <u>both</u> direct and exchange interactions between nucleons. Thus, for scalar meson exchange:

$$\Sigma(k) = ig_s^2\int\frac{d^4q}{(2\pi)^4}\left[\frac{e^{iq^0\epsilon}\mathrm{Tr}G(q)}{m_s^2} + \frac{G(q)}{(k-q)_\mu^2 - m_s^2 + i\epsilon}\right] \tag{28}$$

Vector meson exchange may be included analogously.

Self-consistency is achieved by evaluating the baryon propagator G with Dyson's equation:

$$G(k) = G^0(k) + G^0(k)\Sigma(k)G(k) = \left[\gamma_\mu k^\mu - M - \Sigma(k)\right]^{-1} \tag{29}$$

where $G^0(k)$ is the noninteracting baryon propagator at finite density.[10,14] To

specify the pole structure in G(k), we assume that at finite baryon density, the levels are filled up to $|\underset{\sim}{k}| = k_F$, which implies simple poles with unit residues. The location of the poles then follows from the modified Feynman prescription at finite density, as described in detail in refs. 10 and 14.

Inserting eq. (29) into (28) leads to a set of coupled nonlinear integral equations for $\Sigma^S(k)$, $\Sigma^0(k)$, and $\Sigma^V(k)$. The integrals are finite if we keep only the interactions between the positive-energy valence nucleons.[27] It can then be easily shown that by retaining only the first term in eq. (28), one reproduces the MFT results.[16,14] The HF approximation corrects the MFT for the exchange of identical nucleons within the Fermi sea. The exchange integral also introduces the retarded nature of the interaction. Exchange corrections from the occupied negative-energy Dirac sea are discussed in ref. 28.

The HF integral equations mentioned above are solved in refs. 26 and 27, and the solutions are used to evaluate the HF energy density and EOS. To investigate the size of the corrections, we again perform two comparisons. In table I, we exhibit the new coupling constants determined from a fit to nuclear saturation properties. The changes in g_s and g_v are at the 10% level, which is remarkable, since the HF equations include an additional infinite set of Feynman diagrams, all containing large couplings. The resulting large scalar self-energy $\Sigma^S(k)$ is independent of momentum to $\simeq$ 10% and nearly equal to the MFT result $-g_s\phi_0$; similar behavior is found for the timelike vector piece Σ^0. The three-vector self-energy Σ^V, which modifies the particle momentum according to $\underset{\sim}{k} \to \underset{\sim}{k}\,(1+\Sigma^V)$, is a small correction ($|\Sigma^V| \leq 0.03$) at normal density.

In figs. 7 and 8, we compare the relativistic HF nuclear matter binding energy and EOS with those of the preceding calculations for a fixed set of couplings. (The meson masses are always assigned the values in table I.) The exchange corrections are similar to those from vacuum fluctuations. Although the modifications to the large Lorentz components of the self-energy are small, the effects on the energy/nucleon may be significant. Moreover, although the exchange terms modify the low-density EOS, the corrections to the MFT become small for $\mathcal{E} \gtrsim 0.5$ GeV/fm^3.

Finally, we study the effects of two-nucleon correlations.[29,30] These may be introduced through an effective interaction ("reaction matrix") Γ, which we take to be the solution of the ladder-approximated Bethe-Salpeter equation in the nuclear medium:

$$\Gamma = V + i \int VGG\Gamma \tag{30}$$

Here V is the "ladder" kernel resulting from one-boson exchange, G is the interacting baryon propagator, and we have used the schematic notation of ref. 15.

The single-particle proper self-energy Σ is determined in the present discussion by summing effective direct and exchange interactions between nucleon pairs, which may be written schematically as

$$\Sigma(k) = \sum_{E(k')<E_F} \left[\langle \underset{\sim}{k}\underset{\sim}{k}'|\Gamma|\underset{\sim}{k}\underset{\sim}{k}'\rangle - \langle \underset{\sim}{k}\underset{\sim}{k}'|\Gamma|\underset{\sim}{k}'\underset{\sim}{k}\rangle\right] = -i\int \left[\mathrm{Tr}(G\Gamma) - G\Gamma\right] \tag{31}$$

Self-consistency is again achieved by calculating G through Dyson's equation (29). As before, self-consistency modifies both the single-particle spectrum and the Dirac wave functions.

Equations (29), (30), and (31) may be written in a completely covariant fashion and may be solved in any convenient reference frame. They lead to coupled, nonlinear, multidimensional integral equations that reduce to the familiar "ladder-approximated" Bethe-Salpeter equations in the limit of vanishing baryon density.[15] To render these equations tractable, we make several simplifying approximations.

First, we omit the interactions of positive-energy particles with the negative-energy Dirac sea in the calculation of Σ. This renders eq. (31) finite and corresponds to the procedure used in the MFT and HF approximations. Thus, replacing Γ with V in eq. (31) reproduces the HF result (28). In addition, we reduce the four-dimensional integral implied in eq. (30) to a three-dimensional integral by replacing the full two-particle propagator (iGG) with an approximate, unitarized propagator g.[31] The reaction matrix is then determined by

$$\Gamma = V + \int V g \Gamma \tag{32}$$

Here g must be chosen to maintain two-particle unitarity and the covariance of eq. (30), but is otherwise arbitrary.[30,31]

The solution of eq. (32) can be used to calculate Σ and the procedure iterated to self-consistency. The relativistic HF results show that Σ^S and Σ^0 are reasonably independent of momentum and that $|\Sigma^V| << 1$. We therefore carry out the self-consistency approximately by writing

$$\Sigma(k) \simeq (M^* - M) - \gamma^0 \Sigma^0 \tag{33}$$

where M^* and Σ^0 are constants. This form is analogous to the MFT self-energy. As we will see below, Σ^0 drops out of the self-consistency procedure, and only M^* needs to be determined. Since this parameter enters in G in eqs. (29) and (31) and also in g in eq. (32), the self-consistency procedure is now apparent. One must choose M^* so that the solution to eq. (32), when used in eq. (31), leads to a self-energy Σ that reproduces M^* when approximated as in (33). [The details of this final approximation are described below; see eq. (36).]

For two isolated nucleons, eq. (32) is usually solved in the c. m. frame using the helicity formalism of Jacob and Wick.[32] This is extremely(!) cumbersome to apply at finite density in the frame where the nuclear matter is at rest. Since eq. (32) is covariant, however, we may solve it by Lorentz boosting to the frame in which the total velocity of a given pair of particles is zero (the "center-of-velocity" or c. v. frame).[30] We use velocities rather than momenta, since this eliminates the explicit dependence on the self-energy Σ^μ. Since the nuclear matter is in uniform motion in the c. v. frame, the Fermi sphere is replaced by an ellipsoid, whose shape is determined by k_F and the parameters of the boost.

After boosting to the c. v. frame, one takes matrix elements of eq. (32) between

self-consistent, positive-energy spinors of helicity λ, defined by $U(\underset{\sim}{k},\lambda)$ of eq.(10) with $\underset{\sim}{\sigma}\cdot\underset{\sim}{k}\chi_\lambda = 2\lambda|\underset{\sim}{k}|\chi_\lambda$. These spinors clearly depend on M* and are independent of Σ^μ. One may then project out partial-wave helicity matrix elements[1] $\langle\lambda_1'\lambda_2'|V^J|\lambda_1\lambda_2\rangle$ and $\langle\lambda_1'\lambda_2'|\Gamma^J|\lambda_1\lambda_2\rangle$. If we define the approximate propagator g using the form taken by Blankenbecler and Sugar,[33] eq. (32) takes the form[30]

$$\langle\lambda_1'\lambda_2'|\Gamma^J(p',p;s^*)|\lambda_1\lambda_2\rangle = \langle\lambda_1'\lambda_2'|V^J(p',p)|\lambda_1\lambda_2\rangle$$

$$- \frac{\pi}{2}\sum_{\nu_1\nu_2}\int\frac{k^2\,dk\,dk^0}{(2\pi)^4}\;\frac{\langle\lambda_1'\lambda_2'|V^J(p',k)|\nu_1\nu_2\rangle Q_{av}(k|B)\delta(k^0)}{E^*(k)[\,E^{*2}(k) - s^*/4 - i\varepsilon]}\langle\nu_1\nu_2|\Gamma(k,p;s^*)|\lambda_1\lambda_2\rangle \tag{34}$$

Here p', p, and k denote the magnitudes of the relative three-momenta for the final, initial, and intermediate states in the c. v. frame, and $E^*(k) \equiv (\underset{\sim}{k}^2 + M^{*2})^{1/2}$. Helicities are labeled by λ_i and ν_i, and s* is the Lorentz-invariant square of the total four-velocity (the analogue of the "starting energy" in the usual Brueckner formalism). Q_{av} is an angle-averaged Pauli exclusion operator that prohibits scattering into occupied intermediate states. It is determined by the Fermi "ellipsoid" in the c. v. frame and depends on the baryon current four-vector B_μ in this frame. (Angle averaging is necessary to decouple the partial waves.) Alternative choices for the approximate propagator g are discussed in ref. 14.

Equation (34) is an analogue of the conventional Brueckner-Bethe-Goldstone (BBG) equation.[34] Note that the matrix elements of V^J depend explicitly on Σ through M* contained in the spinors (10). This introduces significant density dependence and differs from the traditional approach in which spinors of fixed mass M are used.[1,2] Moreover, we include the modified wave functions with M* in intermediate states, which is motivated by the large single-particle potentials seen at positive energies in nucleon-nucleus scattering.[6-9] This implies a continuous particle spectrum and an orthogonal set of single-nucleon wave functions.

To achieve self-consistency, Σ must be evaluated in the nuclear matter rest frame. This is done by expanding matrix elements of Γ in terms of Lorentz-invariant amplitudes[7]:

$$\langle\lambda_1'\lambda_2'|\Gamma|\lambda_1\lambda_2\rangle = \langle\lambda_1'\lambda_2'|{}^{S}\Gamma + {}^{V}\Gamma\;\gamma_\mu^{(1)}\gamma^{(2)\mu} + {}^{P}\Gamma\;\gamma_5^{(1)}\gamma_5^{(2)} + {}^{T}\Gamma\;\sigma_{\mu\nu}^{(1)}\sigma^{(2)\mu\nu}$$
$$+ {}^{A}\Gamma\;\gamma_5^{(1)}\gamma_\mu^{(1)}\gamma_5^{(2)}\gamma^{(2)\mu}|\lambda_1\lambda_2\rangle \tag{35}$$

where the superscripts (1) and (2) denote the interacting particles. The five invariant amplitudes ${}^{S}\Gamma$, ..., ${}^{A}\Gamma$ are linear combinations of helicity matrix elements calculated from eq. (34) with $p' = p = (s^*/4 - M^{*2})^{1/2}$, and the advantage of the decomposition (35) is that it is easy to transform these amplitudes back to the nuclear matter rest frame. The self-energy calculated from (31) and (35) is independent of

momentum to within ≈ 10%, and we use $\Sigma(k = k_F)$ to determine a new M* through the relation

$$\Sigma(k)U(\underset{\sim}{k}) = \left[\Sigma^S - \gamma^0\Sigma^0 + \underset{\sim}{\gamma} \cdot \underset{\sim}{k}\,\Sigma^V\right] U(\underset{\sim}{k}) = \left[(\Sigma^S - M^*\Sigma^V) - \gamma^0(\Sigma^0 - E^*(k)\Sigma^V)\right] U(\underset{\sim}{k}) \tag{36}$$

which follows from eq. (10). Comparison with eq. (33) reveals that M* must satisfy $M^* = M + \Sigma^S - M^*\Sigma^V$, with $\Sigma(k)$ evaluated at $k = k_F$. [The final term is a small correction ≈ (0.01)M.] After choosing an M*, the solution of eq. (34) and the resulting $\Sigma(k)$ determines the right-hand side of this relation, leading to a new M*. The procedure is then iterated to self-consistency. (Note that only M* must be determined, since eq. (34) is independent of Σ^u.)

Once the calculation of Γ has converged, the energy follows from the energy-momentum tensor[14,30] and can be written as

$$\mathcal{E} = \sum_{k \leq k_F} \langle \underset{\sim}{k}|\underset{\sim}{\gamma} \cdot \underset{\sim}{k} + M|\underset{\sim}{k}\rangle + \frac{1}{2}\sum_{k',k \leq k_F} \left[\langle \underset{\sim}{k}'\underset{\sim}{k}|\Gamma|\underset{\sim}{k}'\underset{\sim}{k}\rangle - \langle \underset{\sim}{k}'\underset{\sim}{k}|\Gamma|\underset{\sim}{k}\underset{\sim}{k}'\rangle\right] \tag{37}$$

Here the matrix elements involve the spinors of eq. (10), and spin and isospin indices have been suppressed. This result omits contributions from the negative-energy sea and small retardation effects from energy differences between occupied states within the Fermi sea.[27] The pressure may be defined through the thermodynamic relation (17).

We turn now to a discussion of results. All calculations are illustrated for a fixed set of parameters determined in the MFT and given in the first row of table I. Figure 10 compares the self-consistent BBG mass $M^* \approx M + \Sigma^S$ to that obtained in the MFT. It is clear that the single-particle self-energy is modified only slightly by correlations. Similar behavior is found for Σ^0. In fig. 11, we examine the nuclear matter EOS in three different approximations. At low densities, the curves differ because nuclear matter saturates at different densities in each approximation (see figs. 7 and 12). Nevertheless, correlation corrections to the MFT equation of state are small at high densities, and the system smoothly approaches the causal limit.

Figure 12 illustrates several energy/nucleon curves as a function of density. The MFT and self-consistent BBG curves show that correlations produce significant changes in the binding energy, even though they have a small effect on the nucleon self-energy. (Note the different vertical scales in figs. 7 and 12.) The (dash-dot) curve labeled "M* = M" is calculated by neglecting the self-consistency and holding the nucleon mass fixed at M, which essentially corresponds to the treatment in refs. 1 and 2. We emphasize that any calculation (including variational calculations) based on the nonrelativistic ("potential") limit of V will yield similar results, since the nucleon mass is held fixed and the Lorentz character of the interaction is neglected. In contrast, self-consistent wave functions ($M^* \neq M$) have a

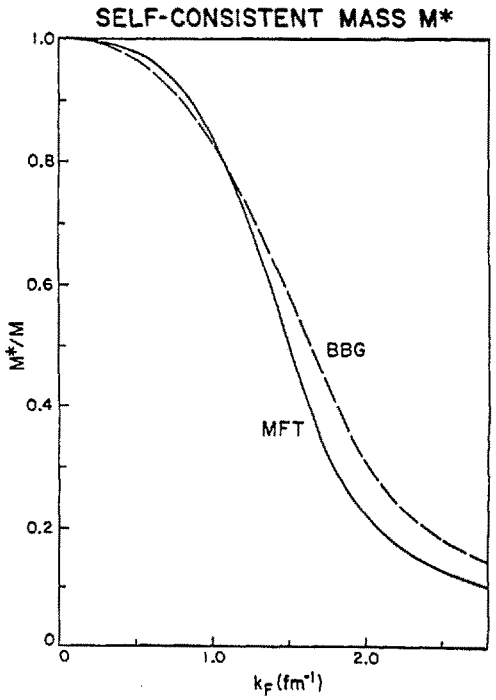

Fig. 10 Self-consistent effective mass M*. Mean-field (solid) and relativistic Brueckner (dashed) results are shown.

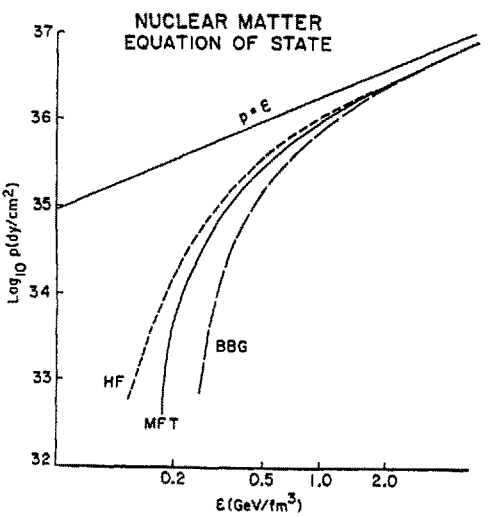

Fig. 11 Nuclear matter equation of state for the mean-field theory (solid), relativistic Hartree-Fock (short dashes), and relativistic Brueckner theory (long dashes). All results use parameters in the first row of table I.

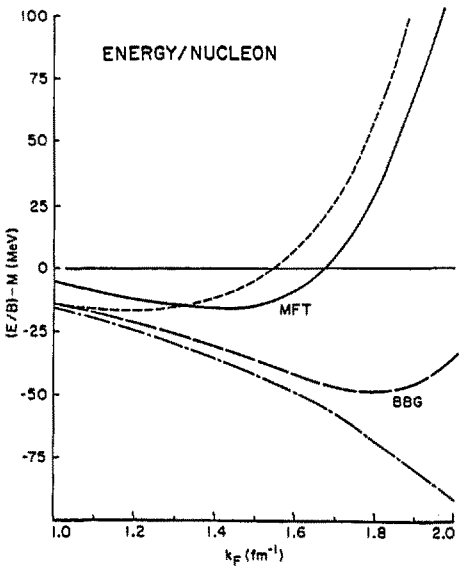

Fig. 12 Energy/nucleon in nuclear matter. Results are for the mean-field theory (solid), relativistic Brueckner theory (long dashes), relativistic Brueckner theory with M* = M (dash-dot), and relativistic Brueckner plus vacuum fluctuations (short dashes). All results use parameters from the first row of table I.

moderate effect at normal densities and become essential at densities two or three times that of equilibrium nuclear matter. The relativistic treatment reduces the attractive part of the interaction as the density increases. As discussed by Day,[35] this trend is precisely what is needed to bring nonrelativistic nuclear matter calculations into better agreement with the empirical saturation point. This suggests that the relativistic approach introduces new physical effects that are important in describing saturation. Additional evidence for this can be seen in the short-dashed curve, in which the vacuum fluctuation correction of eq. (25) is simply added to the BBG result using the self-consistent BBG effective mass. Modifications of the vacuum energy are also omitted in traditional studies of nuclear matter, and it is clear that these contributions may cause significant changes in the binding energy. Variations in the binding energy of a similar magnitude are also found when vertex cutoff factors are inserted (the preceding results involved no such cutoffs) or when alternative choices are made for the unitarized propagator g.[14,29,30] Clearly, much work is needed before we have a detailed understanding of nuclear matter saturation in a consistent relativistic approach.

SUMMARY

Quantum hadrodynamics is a consistent framework for studying the relativistic

nuclear many-body problem. By specifying the interactions with a local, renormalizable lagrangian density, we may include the effects of meson exchange, relativistic propagation, retardation, causality, and the dynamical quantum vacuum. In addition, the correct Lorentz structure of the NN interaction can be maintained.

In this work, we focused on this Lorentz structure using the Walecka model (QHD-I), which incorporates the relevant features of the observed NN force through the exchange of neutral scalar and vector mesons. The Lorentz structure leads naturally to nuclear saturation in the mean-field approximation, and the model parameters were chosen to reproduce empirical saturation properties. The small binding energy of nuclear matter arises from a sensitive cancellation between large attractive and repulsive components in the nucleon self-energy. These large components introduce a new energy scale into the nuclear matter problem and lead to new physical effects from the shifted mass of the nucleon in nuclear matter. They also imply a stiff equation of state for nuclear matter at energy densities greater than approximately 0.5 GeV/fm^3.

The mean-field results were extended to closed-shell nuclei by allowing the meson fields to acquire a spatial variation. This leads to coupled nonlinear differential equations describing nucleons moving in the condensed fields. These equations must be solved self-consistently. The extended model discussed here (QHD-II) contains a minimum number of coupling constants and masses that are again normalized to the bulk properties of nuclear systems. This procedure gives accurate predictions for charge density distributions and rms radii of spherical nuclei. Furthermore, the relativistic Hartree calculations reproduce the observed spin-orbit splittings between single-particle levels and predict the existence of the nuclear shell model.

Because quantum hadrodynamics is a consistent framework, corrections to the MFT may be examined systematically. We studied corrections from vacuum fluctuations, self-consistent nucleon exchange, and two-nucleon correlations. These have a small effect on the large Lorentz scalar and vector components of the baryon self-energy. In addition, corrections to the MFT equation of state become small at energy densities $\mathcal{E} \gtrsim 0.5$ GeV/fm^3. Thus the mean-field approximation provides a simple, accurate description of nuclear matter at densities relevant for neutron stars and energetic heavy ion collisions.

In contrast, the nuclear matter binding energy near equilibrium density involves delicate cancellations and is sensitive to the corrections studied here. The detailed saturation properties of nuclear matter become difficult to calculate in view of the new large energy scale, which suggests that the validity of nonrelativistic nuclear matter calculations be re-examined. An accurate quantitative description of nuclear saturation in a relativistic framework is a challenging topic for future research.

There are other outstanding questions to be addressed in QHD. Of prime importance is the construction of models that incorporate pions accurately, while (hopefully) leaving intact the successes mentioned above. It now appears that some form of chiral symmetry is necessary to achieve a reasonable description of pion-nucleon dynamics

in the nuclear medium.[14,36] Unfortunately, existing chiral models contain strong nonlinearities that pose problems in the description of nuclear matter. This topic requires further investigation.

It is also clear that QHD is an approximation to the underlying quark-gluon structure of nuclear systems. QHD is meant to describe the long-distance behavior of these systems, as studied in low- and medium-energy nuclear physics. By constructing renormalizable QHD theories, the dependence on the intrinsic hadronic structure is minimized. The validity of this dynamical input and the delineation of the boundary between practical QHD and QCD descriptions are important questions for future research.

REFERENCES

1. K. Erkelenz, Phys. Rep. C13, 191 (1974).
2. K. Holinde, Phys. Rep. C68, 121 (1981) and references therein.
3. L.D. Miller, Phys. Rev. C9, 537 (1974); C12, 710 (1975).
4. C.J. Horowitz and B.D. Serot, Nucl. Phys. A368, 503 (1981).
5. J. Boguta, Nucl. Phys. A372, 386 (1981).
6. B.C. Clark, S. Hama, and R.L. Mercer, in Interaction Between Medium Energy Nucleons in Nuclei -- 1982, ed. H. O. Meyer, AIP Conference Proceedings No. 97 (American Institute of Physics, N.Y., 1983), p.260.
7. J. A. McNeil, L. Ray, and S.J. Wallace, Phys. Rev. C27, 2123 (1983).
8. J.A. McNeil, J.R. Shepard, and S.J. Wallace, Phys. Rev. Lett. 50, 1439 (1983); J.R. Shepard, J.A. McNeil, and S.J. Wallace, Phys. Rev. Lett. 50, 1443 (1983).
9. B.C. Clark, S. Hama, R.L. Mercer, L. Ray, and B.D. Serot, Phys. Rev. Lett. 50, 1644 (1983).
10. J.D. Walecka, Ann. Phys. (N.Y.) 83, 491 (1974).
11. J.D. Walecka, in: Nuclear Interactions, Lecture Notes in Physics, vol. 92, ed. B.A. Robson (Springer, Berlin, 1978), p. 294; Nuclear Physics with Electromagnetic Interactions, Lecture Notes in Physics, vol. 108, ed. H. Arenhovel and D. Drechsel (Springer, Berlin, 1979), p. 88.
12. A. Bouyssy and S. Marcos, Phys. Lett. 127B, 157 (1983).
13. B. Frois, Proc. Int'l. Conf. on Antinucleon- and Nucleon-Nucleus Interactions, Telluride, CO, (1985), in press.
14. B.D. Serot and J.D. Walecka, The Relativistic Nuclear Many-Body Problem, Adv. Nucl. Phys. 16, J.W. Negele and E. Vogt, eds. (Plenum, N.Y., 1985), in press.
15. J.D. Bjorken and S.D. Drell, Relativistic Quantum Fields (McGraw-Hill, N.Y., 1965).
16. S.A. Chin, Ann. Phys. (N.Y.) 108, 301 (1977).
17. A.L. Fetter and J.D. Walecka, Quantum Theory of Many-Particle Systems (McGraw-Hill, N.Y., 1971).

18. B.D. Serot, Phys. Lett. 86B, 146 (1979); 87B, 403(E) (1979).
19. B.D. Serot, in: Intersections Between Particle and Nuclear Physics, ed. R.E. Mischke, AIP Conference Proceedings No. 123 (American Institute of Physics, N.Y., 1984). p. 510.
20. A. Bohr and B. Mottelson, Nuclear Structure, vol. I (Benjamin, N.Y., 1969), pp. 324--325.
21. L. Ray and P.E. Hodgson, Phys. Rev. C20, 2403 (1979).
22. R.J. Furnstahl, Proc. LAMPF Workshop on Dirac Approaches to Nuclear Physics, Los Alamos National Laboratory (1985), in press.
23. S.A. Chin and J.D. Walecka, Phys. Lett. 52B, 24 (1974).
24. C.J. Horowitz and B.D. Serot, Phys. Lett. 140B, 181 (1984).
25. B.C. Clark, private communication (1984).
26. M. Jaminon, C. Mahaux, and P. Rochus, Nucl. Phys. A365, 371 (1981).
27. C.J. Horowitz and B.D. Serot, Phys. Lett. 109B, 341 (1982); Nucl. Phys. A399, 529 (1983).
28. A.F. Bielajew and B.D. Serot, Ann. Phys. (N.Y.) 156, 215 (1984).
29. C.J. Horowitz and B.D. Serot, Phys. Lett. 137B, 287 (1984).
30. C.J. Horowitz and B.D. Serot, to be published.
31. R.M. Woloshyn and A.D. Jackson, Nucl. Phys. B64, 269 (1973).
32. M. Jacob and G. Wick. Ann. Phys. (N.Y.) 7, 404 (1959).
33. R. Blankenbecler and R. Sugar, Phys. Rev. 142, 1051 (1966).
34. K.A. Brueckner, C.A. Levinson, and M.H. Mahmoud, Phys. Rev. 95, 217 (1954); H.A. Bethe, Phys. Rev. 103, 1353 (1956); H.A. Bethe and J. Goldstone, Proc. Roy. Soc. (London) A238, 551 (1957); L.C. Gomes, J.D. Walecka, and V.F. Weisskopf, Ann. Phys. (N.Y.) 3, 241 (1958).
35. B.D. Day, Rev. Mod. Phys. 50, 495 (1978); Phys. Rev. Lett. 47, 226 (1981).
36. T. Matsui and B.D. Serot, Ann. Phys. (N.Y.) 144, 107 (1982).
37. I. Sick, J.B. Bellicard, J.M. Cavedon, B. Frois, M. Huet, P. Leconte, P.X. Ho, and S. Platchkov, Phys. Lett. 88B, 245 (1979).
38. B. Frois, J.B. Bellicard, J.M. Cavedon, M. Huet, P. Leconte, P. Ludeau, A. Nakada, Phan Xuan Ho, and I. Sick, Phys. Rev. Lett. 38, 152 (1977).
39. D. Gogny, in: Nuclear Physics with Electromagnetic Interactions, Lecture Notes in Physics, vol. 108, ed. H. Arenhövel and D. Drechsel (Springer, Berlin, 1979), p. 88.